Immunity
Article

The Costimulatory Molecule CD27 Maintains Clonally Diverse CD8$^+$ T Cell Responses of Low Antigen Affinity to Protect against Viral Variants

Klaas P.J.M. van Gisbergen,[1,3,*] Paul L. Klarenbeek,[2] Natasja A.M. Kragten,[1,3] Peter-Paul A. Unger,[1] Marieke B.B. Nieuwenhuis,[1] Felix M. Wensveen,[1] Anja ten Brinke,[4] Paul P. Tak,[2] Eric Eldering,[1] Martijn A. Nolte,[1,3] and Rene A.W. van Lier[1,3]

[1]Department of Experimental Immunology
[2]Department Clinical Immunology and Rheumatology
Academic Medical Center, Meibergdreef 9, 1105 AZ Amsterdam, the Netherlands
[3]Department of Hematopoiesis
[4]Department of Immunopathology
Sanquin Research at CLB and Landsteiner Laboratory, Plesmanlaan 125, 1066 CX Amsterdam, the Netherlands
*Correspondence: k.vangisbergen@sanquin.nl
DOI 10.1016/j.immuni.2011.04.020

SUMMARY

CD70 and CD27 are costimulatory molecules that provide essential signals for the expansion and differentiation of CD8$^+$ T cells. Here, we show that CD27-driven costimulation lowered the threshold of T cell receptor activation on CD8$^+$ T cells and enabled responses against low-affinity antigens. Using influenza infection to study in vivo consequences, we found that CD27-driven costimulation promoted a CD8$^+$ T cell response of overall low affinity. These qualitative effects of CD27 on T cell responses were maintained into the memory phase. On a clonal level, CD27-driven costimulation established a higher degree of variety in memory CD8$^+$ T cells. The benefit became apparent when mice were reinfected, given that CD27 improved CD8$^+$ T cell responses against reinfection with viral variants, but not with identical virus. We propose that CD27-driven costimulation is a strategy to generate memory clones that have potential reactivity to a wide array of mutable pathogens.

INTRODUCTION

CD8$^+$ T cell responses are important in immune defenses against viruses. The generation of CD8$^+$ T cell protection is an intricate process that starts after recognition of viral antigens by expansion and differentiation of naive CD8$^+$ T cells into effector cells. Effector CD8$^+$ T cells produce cytokines including IFN-γ and contain granzyme B and perforin that mediate cytotoxicity. After pathogen elimination, CD8$^+$ T cell memory provides enhanced protection upon reinfection (Harty and Badovinac, 2008; Prlic et al., 2007). The formation of effector and memory cells is a dynamic process, given that a single naive CD8$^+$ T cell can generate a complete CD8$^+$ T cell response (Gerlach et al., 2010; Stemberger et al., 2007). Effector CD8$^+$ T cells that develop into memory cells may already separate from effector cells during the first cell division (Chang et al., 2007) and CD8$^+$ T cells may have fully developed memory potential at early time points that precede the peak of the primary CD8$^+$ T cell response (Badovinac et al., 2005; Kedzierska et al., 2007). Memory precursors are typified by expression of CD127 and fall into distinct subsets that will form CD62L$^+$ central and CD62L$^-$ effector memory CD8$^+$ T cells (Huster et al., 2004; Kaech et al., 2003).

A prerequisite for efficient CD8$^+$ T cell responses is that individual effector cells are of sufficient antigen affinity. Generation of high-affinity CD8$^+$ T cell responses occurs through a selection process in which clones of high antigen affinity have a competitive advantage over low-affinity ones (Butz and Bevan, 1998; Smith et al., 2000). We described that apoptosis regulated through the Noxa and Mcl-1 axis plays an essential role in survival of the fittest T cell clones (Wensveen et al., 2010). Although high antigen affinity is required for effector T cells, the selection of only high-affinity clones may be less desirable for memory T cells. Memory may be important not only for protection against identical pathogens, but also for protection against mutated pathogens (Brehm et al., 2002; Haanen et al., 1999). For ensuring the presence of cross-protective memory, the maintenance of a large repertoire of CD8$^+$ T cell clones into the memory compartment will be advantageous. However, the underlying mechanisms that enable the maintenance of clonal diversity are unclear.

The two-signal theory dictates that T cell responses depend on both antigen and costimulation (Lenschow et al., 1996). The main costimulatory pathways are mediated by CD80 and CD86 that bind CD28 and by members of the tumor necrosis factor (TNF) and TNF receptor superfamily, such as CD70 and CD27 (Acuto and Michel, 2003; Croft, 2009; Nolte et al., 2009). CD27 provides, upon binding of its unique ligand CD70, an essential pathway of costimulation for CD8$^+$ T cell responses in vivo (Hendriks et al., 2000). Immune activation induces expression of CD70 on T and B cells and on a subset of DCs that require CD70 to stimulate naive CD8$^+$ T cells (Belz et al., 2007). CD27 is expressed on naive CD8$^+$ T cells and mediates proliferation, survival and differentiation of activated CD8$^+$ T cells (Croft,

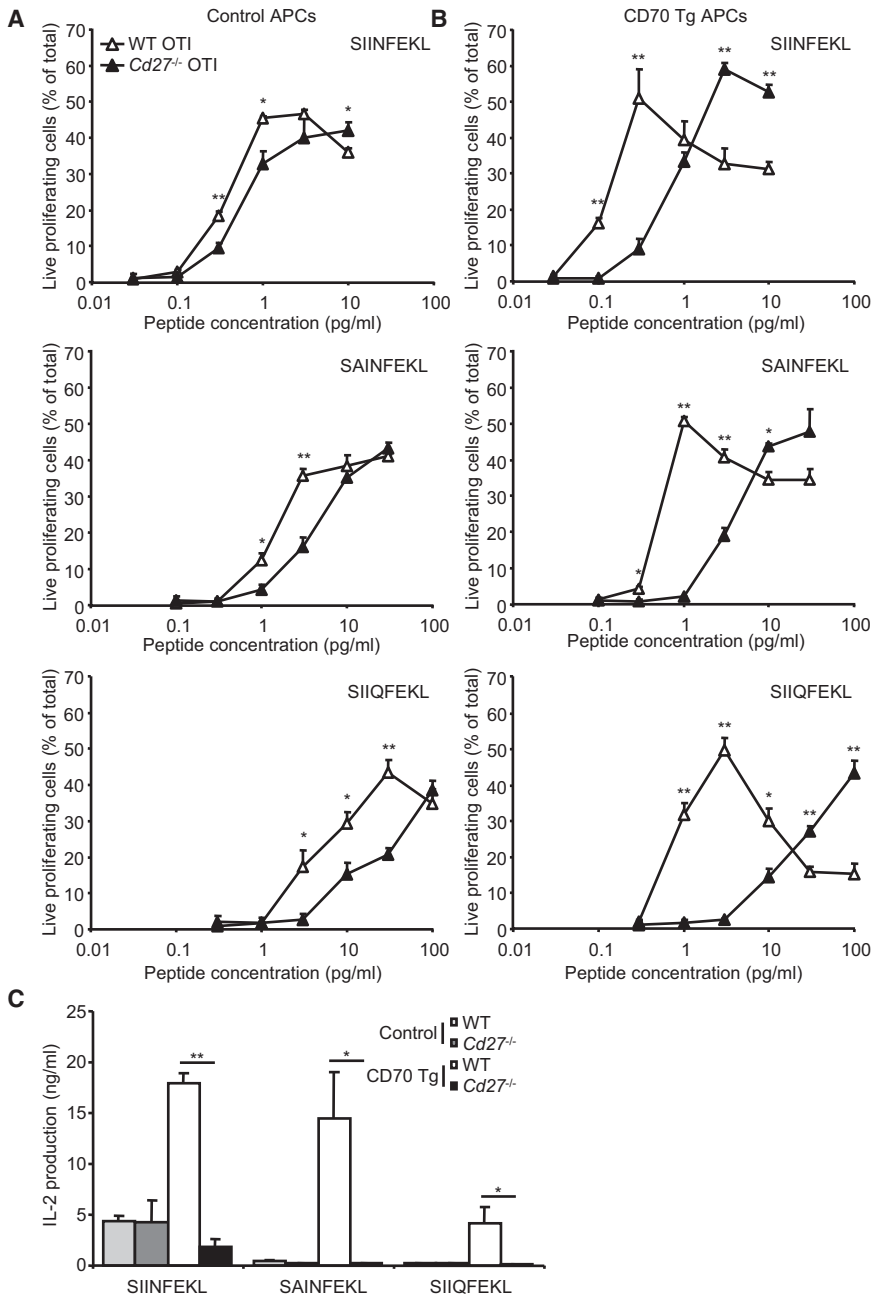

Figure 1. Antigen Density and Avidity Determine the Outcome of CD27-Driven Costimulation

(A and B) WT and *Cd27*$^{-/-}$ OTI cells were stimulated with peptide for 3 days in the presence of irradiated splenocytes of (A) *Cd27*$^{-/-}$ mice (control APCs) or (B) *Cd27*$^{-/-}$ × CD70 Tg mice (CD70 Tg APCs). Proliferation and survival was quantified by determining the percentage of CFSE^{lo} and PI^{lo} cells of total OTI cells after stimulation with the peptides SIINFEKL (top panels), SAINFEKL (center panels), and SIIQFEKL (bottom panels).

(C) IL-2 production was measured using ELISA in supernatants of WT and *Cd27*$^{-/-}$ OTI cells that had been stimulated for 3 days with 10 pg/ml of the indicated peptides in the presence of control APCs or CD70 Tg APCs. Representative data is shown of three separate experiments. Error bars denote standard error of the mean (SEM). See also Figure S1.

RESULTS

The Costimulatory Effect of CD70 Depends upon Antigen Density and Avidity

For testing whether antigenic strength affected costimulation through CD27, OTI TCR Tg CD8$^+$ T cells were stimulated with graded concentrations of the high-affinity peptide SIINFEKL in the presence of APCs expressing either low amounts of endogenous CD70 (control APCs) or high amounts of transgenic CD70 (CD70 Tg APCs; Figure S1A available online). These APCs did not differ in expression of MHC class I or other costimulatory molecules (Figure S1B). CD27 induced expansion of dividing OTI cells when low amounts of peptide were present (Carr et al., 2006; Peperzak et al., 2010), but provoked cell death of dividing OTI cells when the amount of peptide was high (Figures 1A and 1B; Figure S1C). The costimulatory effects were mediated by CD27 and CD70, as they were diminished in the presence of control APCs and absent when CD27-deficient OTI cells were used (Figures 1A and 1B). For comparison of low versus high avidity stimulation, previously described peptide variants of SIINFEKL were used (Zehn et al., 2009). CD27 induced similar effects upon stimulation with the low avidity peptides SAINFEKL and SIIQFEKL, albeit at higher peptide concentrations (Figures 1A and 1B; Figure S1D). The costimulatory effect of CD27 relatively increased, when OTI cells were stimulated with peptides of lower avidity (Figures 1A and 1B; Figure S1D). Importantly, under conditions in which CD27 induced cell death of OTI cells stimulated with high avidity SIINFEKL peptide, CD27 enhanced expansion of OTI cells stimulated with the lower avidity peptides (Figures 1A and 1B;

2009; Nolte et al., 2009). The dependence on costimulation may not be absolute as the requirement for e.g., CD28 is dependent on the duration and the level of antigenic triggering (Acuto and Michel, 2003; Kündig et al., 1996).

It is unknown whether the impact of CD27-driven costimulation is dependent on the strength of antigenic stimulation. We here tested whether CD27-driven costimulation influenced competition between CD8$^+$ T cell clones of distinct affinity within polyclonal CD8$^+$ T cell responses. We found that CD27 provided selective advantages for the maintenance of low-affinity CD8$^+$ T cells and thereby elevated the clonal diversity of CD8$^+$ T cell responses. Importantly, we demonstrate that this was beneficial upon subsequent encounter with variant virus.

Figure S1D). CD27-driven costimulation also increased IL-2 production of OTI cells after stimulation with SIINFEKL, as previously published (Peperzak et al., 2010), and after stimulation with the low-avidity peptides (Figure 1C). In summary, low-avidity CD8+ T cells were more dependent on CD27-driven costimulation than high-avidity CD8+ T cells.

CD27 Decreases the Antigen Affinity of Influenza-Specific CD8+ T Cells

For studying the effect of CD27-driven costimulation during CD8+ T cell responses in vivo, WT and *Cd27*$^{-/-}$ mice were infected with the influenza virus strain A/PR8/34. CD8+ T cell responses developed in mediastinal (m)LN, spleen and lungs of both WT and *Cd27*$^{-/-}$ mice (Figure 2A). In the absence of CD27, numbers of influenza-specific CD8+ T cells were higher within the lungs and to a lesser extent within the spleen (Figure 2A). Comparable results were obtained with the influenza virus strain HK2/68 that contains a distinct dominant epitope (Figure 2B). Analysis of total CD8+ T cells for effector markers revealed no differences between WT and *Cd27*$^{-/-}$ mice, indicating that overall effector formation was comparable (Figure S2). Because CD27 was not essential for the generation of CD8+ T cell responses after influenza infection, we could question whether the avidity-dependent effects of CD27-driven costimulation observed in vitro would occur during influenza infection. As an approximate measure of antigen affinity, we determined the amount of tetramer binding on a per-cell basis. Influenza-specific CD8+ T cells of *Cd27*$^{-/-}$ spleen had a higher MFI of tetramer binding at the peak of the response than those of WT spleen (Figures 2C and 2D). Similarly, the MFI of tetramer binding was higher in influenza-specific CD8+ T cells of mLNs and lungs of *Cd27*$^{-/-}$ mice (Figure 2D). These findings could not be explained by the expression levels of the TCR-$\alpha\beta$ and CD3 complex, which were comparable between both mice strains (Figure 2E).

To further examine whether variations in affinity induced differences in tetramer binding, we performed tetramer binding in the presence of increasing concentrations of blocking tetramer antibodies. Inhibition of tetramer binding was observed at lower concentrations of tetramer antibodies in influenza-specific CD8+ T cells of WT mice compared to those of *Cd27*$^{-/-}$ mice (Figure 2F), corroborating the results on the MFI of tetramer binding. We performed peptide titrations to obtain a separate measure of antigen affinity. IFN-γ responses of WT and *Cd27*$^{-/-}$ mice were similar in magnitude upon restimulation with an optimal peptide dose (Figure 2G), but influenza-specific CD8+ T cells of *Cd27*$^{-/-}$ mice produced IFN-γ at lower doses of peptide than those of WT mice (Figure 2H). We concluded that CD27 decreased the average affinity for antigen of influenza-specific CD8+ T cells.

CD27 Enables Low-Affinity CD8+ T Cells to Differentiate into Effectors

CD8+ T cells differentiate into different subsets of effector CD8+ T cells upon primary infection (Kaech et al., 2003). Effector memory (EM)-type memory precursor effector cells (MPECs) appeared relatively late in the CD8+ T cell response of WT mice and were only detectable at day 8 within the mLN and at day 10 within the spleen (Figures 3A–3C; Figure S3A), which is near the peak of the total CD8+ T cell response (Figure S3B). EM-type MPEC formation was specifically diminished in mLN and spleen of *Cd27*$^{-/-}$ mice at these time points (Figures 3A–3C; Figure S3A). Differences in antigen encounter could have influenced CD8+ T cell differentiation, but this was unlikely, given that we did not observe differences in expression of antigen-induced molecules such as CD43 (Figure S3C) and CD25 (Figure S3D). Moreover, viral clearance within the lungs was similar between WT and *Cd27*$^{-/-}$ mice, indicating that antigen load was not the cause of the observed differences in CD8+ T cell differentiation (Figure S3E). Thus, EM-type MPECs, in contrast to central memory (CM)-type MPECs and short-lived effector cells (SLECs), require CD27 at least in part for formation or maintenance.

We were interested in the antigen affinity of the different effector CD8+ T cell subsets. The MFI of tetramer binding within both the SLEC and the EM-type MPEC compartment of effector CD8+ T cells, but not within CM-type MPECs, was increased in *Cd27*$^{-/-}$ mice (Figure 3D). In both WT and *Cd27*$^{-/-}$ mice, CM-type MPECs bound lower amounts of tetramer than EM-type MPECs and SLECs (Figure 3D), suggesting that CD27 induced a shift in the repertoire of influenza-specific CD8+ T cells of high affinity toward low affinity, in particular in the EM-type MPEC and SLEC compartment. By setting arbitrary gates for low and high tetramer binding (Figure 2C), we observed an increase in high tetramer binding influenza-specific CD8+ T cells and a decrease in low tetramer binding CD8+ T cells in the absence of CD27 (Figure 3E). *Cd27*$^{-/-}$ mice had fewer low tetramer binding EM-type MPECs and SLECs and increased numbers of high tetramer binding SLECs compared to WT mice (Figure 3E). Taken together, these findings show that CD27-driven costimulation alleviated antigenic competition, given that it allowed survival and effector differentiation of low-affinity CD8+ T cell clones at the expense of high-affinity CD8+ T cell clones.

CD8+ T Cells Require CD27 in a Cell-Autonomous Fashion

Because CD27 expressed on CD4+ T cells is important for T cell help in CD8+ T cell responses (Xiao et al., 2008), we tested whether the above depicted differences were a direct or indirect consequence of CD27 ligation on CD8+ T cells. Mixed BM chimeras were made by reconstituting lethally irradiated WT recipients with a 1:1 mixture of WT and *Cd27*$^{-/-}$ donor BM. After reconstitution of the hematopoietic compartment, mice were infected with A/PR8/34. BM chimeric mice had similar numbers of WT and *Cd27*$^{-/-}$ donor-derived total (Figure S4A) and influenza-specific CD8+ T cells (Figure 4A), but EM-type MPECs were lower in the *Cd27*$^{-/-}$ donor compartment (Figure 4A). Moreover, influenza-specific CD8+ T cells of *Cd27*$^{-/-}$ donor origin bound higher amounts of tetramer than those of WT donor origin (Figures 4B and 4C). Thus, CD27 on CD8+ T cells mediated formation or maintenance of EM-type MPECs and low-affinity effector CD8+ T cells. These results also established that CD8+ T cell-extrinsic factors such as viral and antigenic load and antigen presentation did not cause differences between WT and *Cd27*$^{-/-}$ mice.

Peperzak et al. (2010) showed that CD27 regulates IL-2 production in CD8+ T cells and that CD27-induced IL-2 is required for CD8+ T cell survival at tissue sites. To establish whether CD27 also induced cytokine production in CD8+ T cell responses against A/PR8/34, we measured cytokine production in CD8+ T cells after restimulation. IFN-γ production was similar

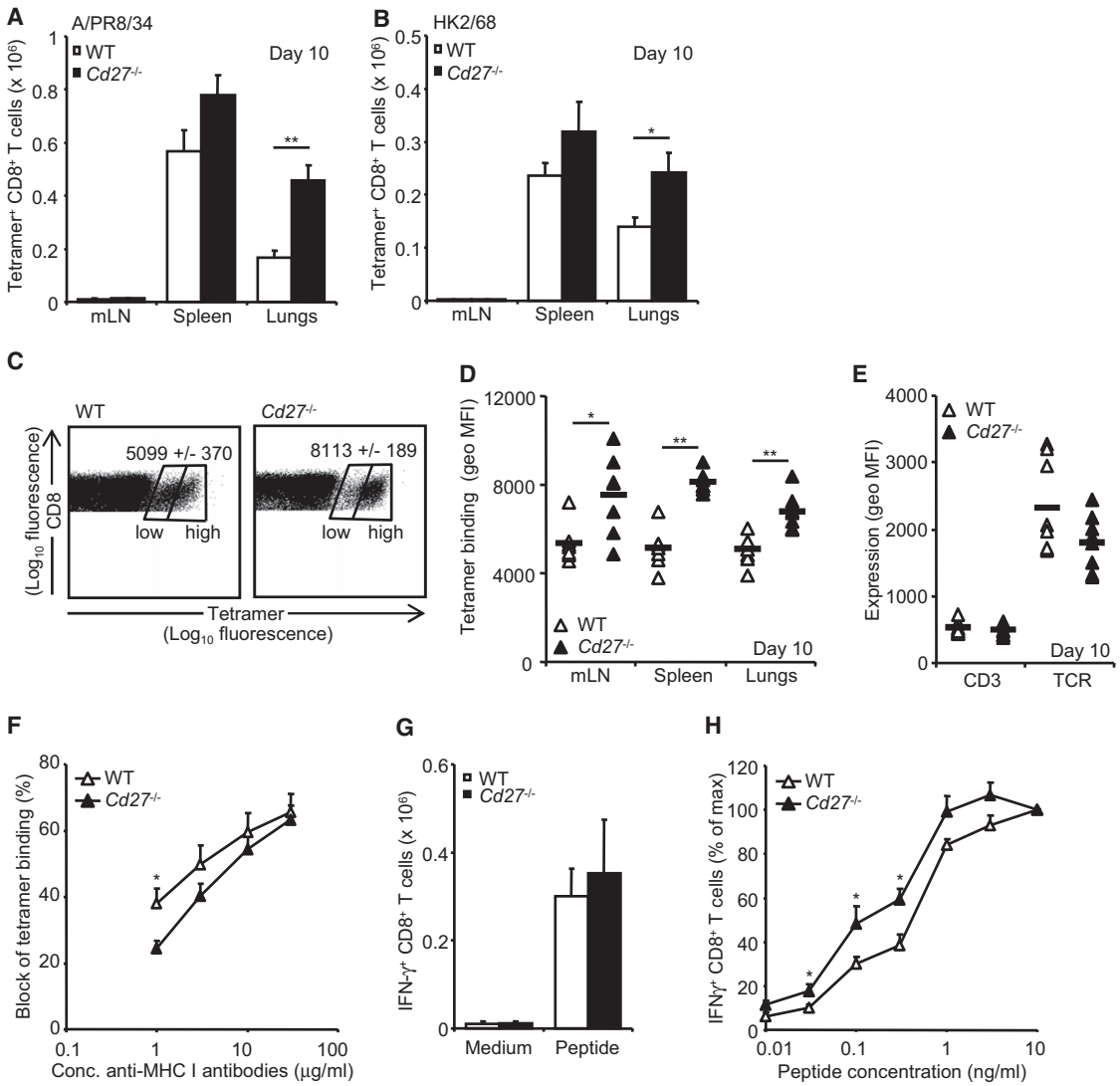

Figure 2. CD27 Lowers the Affinity of the Virus-Specific CD8+ T Cell Population

(A and B) WT and *Cd27*$^{-/-}$ mice were infected with (A) A/PR8/34 or (B) HK2/68 and after 10 days influenza-specific CD8+ T cells were enumerated in mLN, spleen and lungs with (A) A/PR8/34 or (B) HK2/68 specific tetramers.

(C–H) WT and *Cd27*$^{-/-}$ mice were infected with A/PR8/34 and sacrificed 10 days later for analysis.

(C) Representative dot plots display CD8+ T cells of WT and *Cd27*$^{-/-}$ spleen that are labeled for CD8 and tetramer. Insets denote the mean ± SEM of the geo MFI of the tetramer+ CD8+ T cells of WT (left) and *Cd27*$^{-/-}$ mice (right). The difference in geo MFI is significant between WT and *Cd27*$^{-/-}$ mice ($p < 0.005$). Arbitrary gates indicate low and high tetramer binding CD8+ T cells.

(D) Quantification of the geo MFI of tetramer binding of tetramer+ CD8+ T cells of mLN, spleen and lungs of WT and *Cd27*$^{-/-}$ mice.

(E) Geo MFI of CD3 and TCR-β expression of influenza-specific CD8+ T cells of WT and *Cd27*$^{-/-}$ spleen.

(F) Splenocytes of WT and *Cd27*$^{-/-}$ mice were labeled with tetramers in the presence of increasing concentrations of blocking tetramer antibodies. The block in tetramer binding, compared to tetramer binding in the absence of blocking antibodies, is displayed.

(G) Splenocytes of WT and *Cd27*$^{-/-}$ mice were briefly cultured with or without peptide and the absolute number of CD8+ T cells that produced IFN-γ was determined.

(H) The relative percentage of IFN-γ producing CD8+ T cells in spleen of WT and *Cd27*$^{-/-}$ mice is shown upon restimulation of increasing concentrations of peptide. The percentage of IFN-γ producing CD8+ T cells in the presence of 10 ng/ml peptide was set at 100%. Error bars denote standard error of the mean (SEM). See also Figure S2.

between WT and *Cd27*$^{-/-}$ mice (Figure 2G), but production of IL-2 was diminished in *Cd27*$^{-/-}$ mice (Figures 4D and 4E). Similar results were obtained with HK2/68 containing a distinct dominant epitope (Figure S4B–S4D). Expression of IL-2 by IFN-γ-producing CD8+ T cells was also reduced in influenza-specific donor CD8+ T cells of *Cd27*$^{-/-}$ origin in mixed BM chimeric mice (Figure 4F). Thus, signaling through CD27 on CD8+ T cells also induced IL-2 production in immune responses, in which CD27 was largely dispensable for expansion of CD8+ T cells. By providing IL-2, CD27-driven costimulation may lower

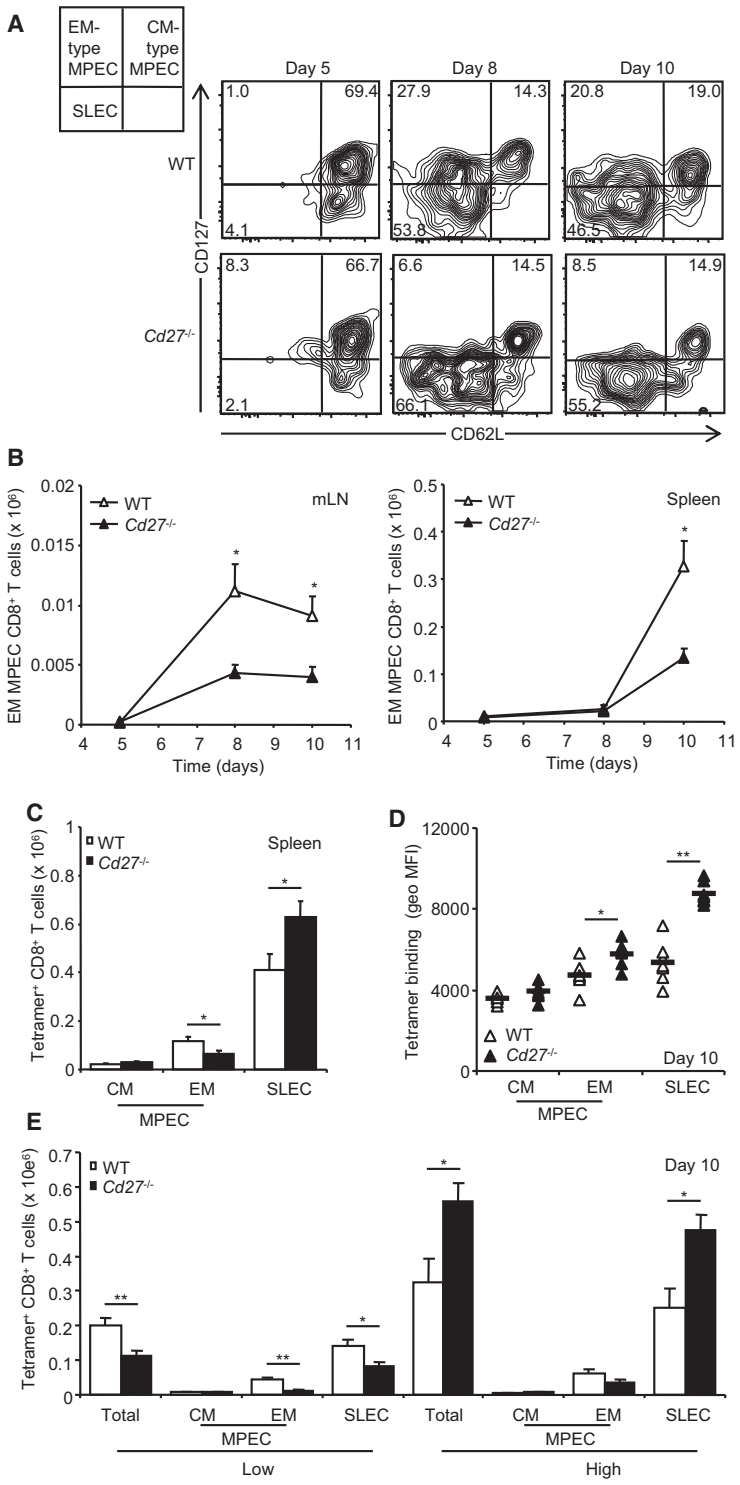

Figure 3. CD27 Restricts Effector Differentiation of Low- but Not High-Affinity CD8+ T Cells

(A–C) The phenotype of influenza-specific CD8+ T cells was analyzed in the mLN and spleen of A/PR8/34-infected mice using CD127 and CD62L.

(A) Representative dot plots display tetramer+ CD8+ T cells labeled for CD62L and CD127 in the mLN of 5 day-, 8 day-, and 10 day-infected WT (top) and *Cd27*$^{-/-}$ mice (bottom). Insets denote the percentage of influenza-specific CD8+ T cells within the respective quadrants.

(B) The absolute number of EM-type MPEC CD8+ T cells was quantified at day 5, 8, and 10 in the mLN (left panel) and spleen (right panel).

(C) Influenza-specific CD8+ T cell effector subsets in spleen of WT and *Cd27*$^{-/-}$ mice were quantified at day 10.

(D) The geo MFI of tetramer binding was determined in the indicated influenza-specific CD8+ T cell effector subsets of spleen of WT and *Cd27*$^{-/-}$ mice.

(E) The absolute numbers of total, CM-type MPEC, EM-type MPEC and SLEC phenotype CD8+ T cells with high and low tetramer binding were determined within the spleen of WT and *Cd27*$^{-/-}$ mice. See also Figure S3.

the threshold for CD8+ T cells to expand after antigenic challenge and maintain low-affinity CD8+ T cell clones.

Low-Affinity CD8+ T Cells Require CD27 to Develop into Memory Cells

Next, we investigated whether the CD27-dependent differences in TCR affinity of primary CD8+ T cells would translate into the memory phase. The size of the memory CD8+ T cell pool in the mLN and spleen of WT and *Cd27*$^{-/-}$ mice was comparable at day 28 after infection (Figure 5A), although a significant increase in influenza-specific CD8+ T cells was still present within the lungs (Figure 5A). Thus, the small compartment of EM-type MPEC CD8+ T cells in *Cd27*$^{-/-}$ mice during primary infection did not result in lower numbers of bona fide memory CD8+ T cells. Furthermore, no phenotypic differences between WT and *Cd27*$^{-/-}$ mice regarding expression of CD127 and CD62L (Figure S5A) or CD127 and CD43 (Figure S5B) on memory CD8+ T cells were found. However, similar to effector CD8+ T cells during the primary response, memory CD8+ T cells were of higher affinity in the absence of CD27-driven costimulation (Figures 5B and 5C). The differences between WT and *Cd27*$^{-/-}$ mice were most pronounced within the EM-type compartment of memory CD8+ T cells (Figure 5D) and a specific decrease in the low tetramer binding compartment of influenza-specific EM CD8+ T cells of *Cd27*$^{-/-}$ was apparent (Figure 5E). Thus, low-affinity CD8+ T cells, in contrast to high-affinity CD8+ T cells, required CD27 for maintenance in the memory compartment.

Clonal Diversity of CD8+ T Cell Memory Is Enhanced by CD27-Driven Costimulation

The CD8+ T cell response against the $NP_{366-374}$ epitope of influenza is for a large part restricted to Vβ8.3 (Kedzierska et al., 2004). Vβ8.3+ CD8+ T cells bound higher amounts of tetramer than other influenza-specific CD8+ T cells (Figure 6A), indicating that they are of superior antigen affinity. A higher percentage of influenza-specific CD8+ T cells of *Cd27*$^{-/-}$ mice expressed Vβ8.3 compared to WT mice (Figures 6B–6D). This difference was not present in noninfected mice, nor in the nontetramer population of influenza-infected mice (Figure S6A). A higher usage of Vβ8.3 was

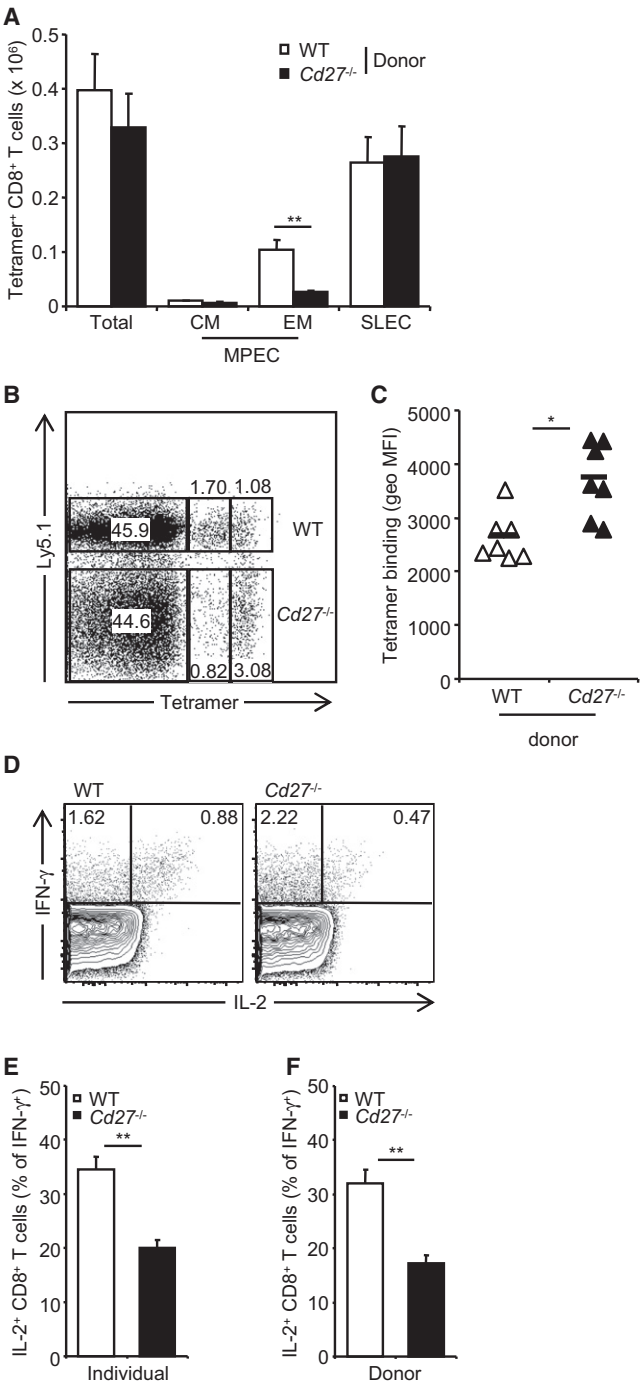

Figure 4. CD27 Regulates CD8+ T Cells in a Cell-Intrinsic Manner

(A–C) Mixed BM chimeras that contained WT and *Cd27*$^{-/-}$ donor BM were infected with A/PR8/34 and sacrificed 10 days later.

(A) Total numbers and numbers of the indicated subsets of tetramer$^+$ CD8$^+$ T cells of WT and *Cd27*$^{-/-}$ donors were determined in spleen.

(B) Representative dotplot displays tetramer binding of splenic Ly5.1$^+$ WT and Ly5.1$^-$ *Cd27*$^{-/-}$ donor CD8$^+$ T cells.

(C) The mean of tetramer binding to influenza-specific CD8$^+$ T cells of WT and *Cd27*$^{-/-}$ donor origin was determined in spleen.

(D–F) Splenocytes of WT, *Cd27*$^{-/-}$, and mixed BM chimeric mice that had been infected with A/PR8/34 10 days previously were re-stimulated with peptide.

observed in influenza-specific CD8$^+$ T cells of *Cd27*$^{-/-}$ mice at early and memory time points of infection (Figure 6C), at all tissue sites analyzed (Figures 6B–6D), in both EM-type MPECs and SLECs, but not in CM-type MPECs (Figure S6B), nor in BM chimeric mice (Figure S6C). This correlated with the increase in tetramer binding in *Cd27*$^{-/-}$ mice and strongly suggested that CD27 counteracted the selection of the Vβ8.3-restricted repertoire of influenza-specific CD8$^+$ T cells to enhance clonal diversity. In contrast to infection with A/PR8/34, HK2/68 induced increased numbers of high tetramer binding Vβ11$^+$ clones within the influenza-specific CD8$^+$ T cell population of *Cd27*$^{-/-}$ mice (Figures S6D–S6F). Thus, although differences between the A/PR8/34 and HK2/68 $NP_{366-374}$ epitopes impacted Vβ usage and provided very different settings, CD27-driven effects were highly comparable during both infections.

We next addressed whether CD27 also enhanced diversity at the level of the clonal repertoire by using high throughput sequencing (Klarenbeek et al., 2010), which allowed the analysis of up to 10,000 clones per mouse. We focused on the Vβ8.3 family and analyzed tetramer$^+$ CD8$^+$ T cells of WT and *Cd27*$^{-/-}$ mice at 28 days after infection. Approximately 75 different clones per mouse contributed to the $NP_{366-374}$ and Vβ8.3 restricted segment of the influenza-specific CD8$^+$ T cell response (Figure 6E), and the number of distinct clones was not different between WT and *Cd27*$^{-/-}$ mice (Figure 6E). However, when clonal distribution was analyzed, the contribution of dominant clones was greater in *Cd27*$^{-/-}$ mice (Figure 6F; Figure S6G). Moreover, the number of subdominant clones with a contribution of more than 1% to the total pool of clones was larger in WT mice than in *Cd27*$^{-/-}$ mice (Figure 6F; Figure S6H). The clonal analysis therefore revealed an additional layer of CD27-driven diversity in influenza-specific CD8$^+$ T cell responses.

The Vβ8.3-restricted CD8$^+$ T cell response to the $NP_{366-374}$ epitope is for a large part public (Kedzierska et al., 2004), and indeed, three of the more dominant clones were found in all of the mice (Figure 6F; Table S1). The three most dominant clones of *Cd27*$^{-/-}$ mice were consistently public, whereas this was not the case for WT mice (Figure 6F). Furthermore, the combined abundance of public clones within the influenza-specific CD8$^+$ T cell pool was much higher in *Cd27*$^{-/-}$ mice than in WT mice (Figure 6F; Figure S6I). Interestingly, the public clone with the SGGA motif, which previously has been shown to be of lower affinity than the other public clones (Kedzierska et al., 2008), was not more abundant in *Cd27*$^{-/-}$ mice compared to WT mice (Figure 6F). Thus, CD27-driven costimulation induced a more diverse influenza-specific TCR repertoire by enabling more nonpublic clones to establish a higher degree of dominance. This may strongly increase clonal diversity of CD8$^+$ T cell memory at the population level and could allow individuals to generate overlapping but distinct memory CD8$^+$ T cell responses.

(D) Representative dotplots display intracellular staining of CD8$^+$ T cells of WT (left) and *Cd27*$^{-/-}$ mice (right) for IFN-γ and IL-2. Insets denote the percentage of CD8$^+$ T cells within the respective quadrants.

(E and F) The percentage of IL-2 coproducing CD8$^+$ T cells within the IFN-γ-producing population was determined in (E) WT and *Cd27*$^{-/-}$ mice and (F) BM chimeric mice containing WT and CD27 donor BM. Error bars denote standard error of the mean (SEM). See also Figure S4.

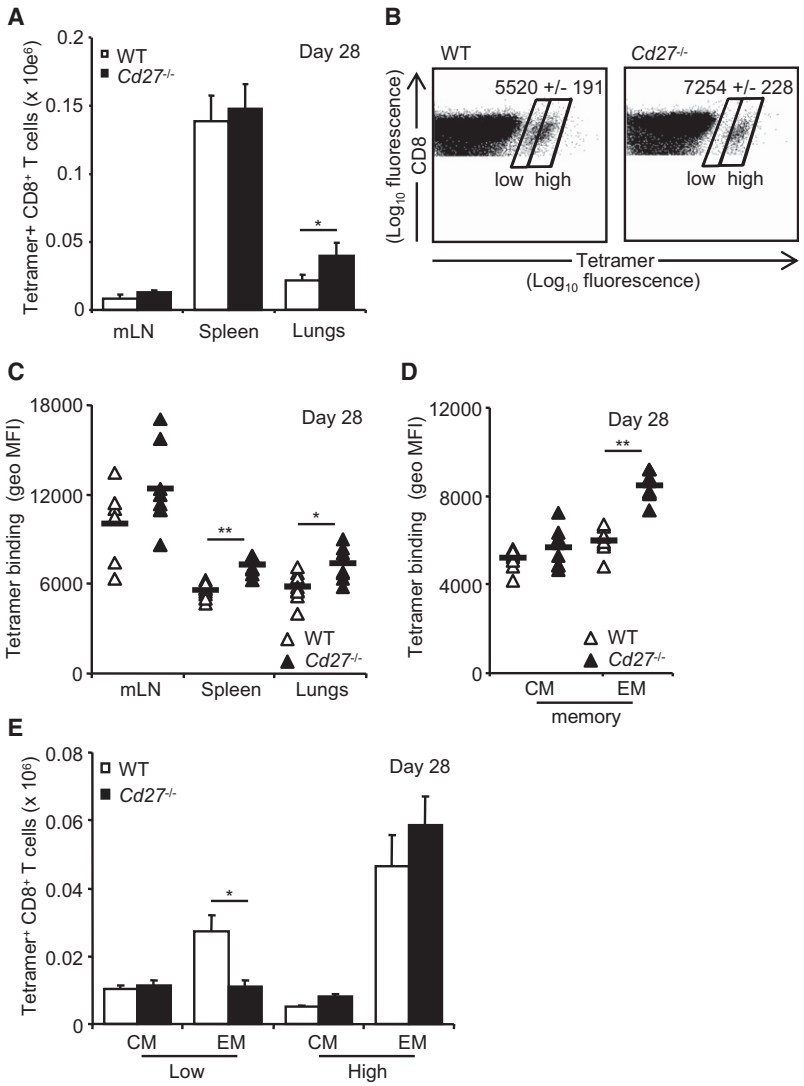

Figure 5. CD27 Ensures the Presence of Low-Affinity Clones in the Memory CD8+ T Cell Pool

WT and *Cd27*$^{-/-}$ mice were infected with A/PR8/34 and 28 days later influenza-specific CD8+ T cells were analyzed.

(A) Absolute numbers of influenza-specific CD8+ T cells were determined in the mLN, the spleen, and lungs of WT and *Cd27*$^{-/-}$ mice.

(B) Representative dot plots are shown that display tetramer binding of CD8+ T cells of spleen of WT and *Cd27*$^{-/-}$ mice. Insets denote geo MFI +/- SEM of tetramer binding to influenza-specific CD8+ T cells. The difference in geo MFI is significant between WT and *Cd27*$^{-/-}$ mice ($p < 0.005$). Arbitrary gates indicate low and high tetramer binding CD8+ T cells.

(C) The geo MFI of tetramer binding was determined in influenza-specific CD8+ T cells of the mLN, the spleen, and lungs of WT and *Cd27*$^{-/-}$ mice.

(D) Similarly, the geo MFI of tetramer binding was determined in the indicated memory subsets of influenza-specific CD8+ T cells of WT and *Cd27*$^{-/-}$ spleen.

(E) The absolute numbers of CM and EM CD8+ T cells with high and low tetramer binding were determined within the spleen of WT and *Cd27*$^{-/-}$ mice. Error bars denote standard error of the mean (SEM). See also Figure S5.

CD27 Enhances CD8+ T Cell Responses against Heterologous Rechallenge

CD27-initiated maintenance of low-affinity CD8+ T cells in the primary response and the memory phase appears countereffective, given that these clones are not expected to mediate strong protection upon rechallenge with the same virus. However, memory CD8+ T cells may also provide enhanced protection against heterologous pathogens, such as upon rechallenge with viruses carrying mutated epitopes (Haanen et al., 1999). Therefore, CD8+ T cell responses after sequential infection with the heterologous viruses HK2/68 and A/PR8/34 were studied. In line with previous findings (Cornberg et al., 2006), the repertoire of heterologous recall responses was more limited than that of homologous recall responses and did not contain any of the public clones (Figures S7A–S7C). This suggested that heterologous CD8+ T cell recall responses rely on cross-reactive clones that are more likely to be present in a diverse memory repertoire. On the basis of the above described findings, we predicted that CD27 was involved in the maintenance of such cross-reactive CD8+ T cell clones. Indeed, *Cd27*$^{-/-}$ mice had lower secondary CD8+ T cell responses than WT mice after heterologous rechallenge (Figure 7A), but did not have reduced secondary CD8+ T cell responses after rechallenge with an influenza virus containing the same dominant CD8+ T cell epitope (Figure 7B). Thus, CD27 specifically promoted secondary CD8+ T cell responses against heterologous, but not homologous influenza viruses.

We tested whether CD8+ T cells were cross-reactive after rechallenge with heterologous influenza virus by using simultaneous labeling with tetramers containing peptides of either virus strain. Both WT and *Cd27*$^{-/-}$ mice contained cross-reactive clones, but WT mice displayed a significantly higher degree of cross-reactive CD8+ T cells (Figure 7C). To examine whether CD27 controlled the maintenance of cross-reactive CD8+ T cell clones before rechallenge, we followed influenza-specific CD8+ T cells of HK2/68 infected mice. Already after primary infection, influenza-specific CD8+ T cells were present that recognized the modified peptide corresponding to that of the A/PR8/34 virus, but to a lesser extent than influenza-specific CD8+ T cells recognizing the native HK2/68 peptide (Figures 7D–7F). Native tetramer responses were equal between WT and *Cd27*$^{-/-}$ mice (Figure 7D), whereas cross-reactive tetramer responses were strongly reduced in *Cd27*$^{-/-}$ mice at all time points (Figure 7E). After restimulation, the number of influenza-specific CD8+ T cells that recognized the peptide of both HK2/68 and A/PR8/34 were reduced in *Cd27*$^{-/-}$ mice (Figures 7D and 7E). Thus, CD27-driven costimulation ensured the maintenance of cross-reactive CD8+ T cell clones during primary infection and into the memory phase. This may prove useful in future encounters with a broad array of distinct yet similar pathogens. Such

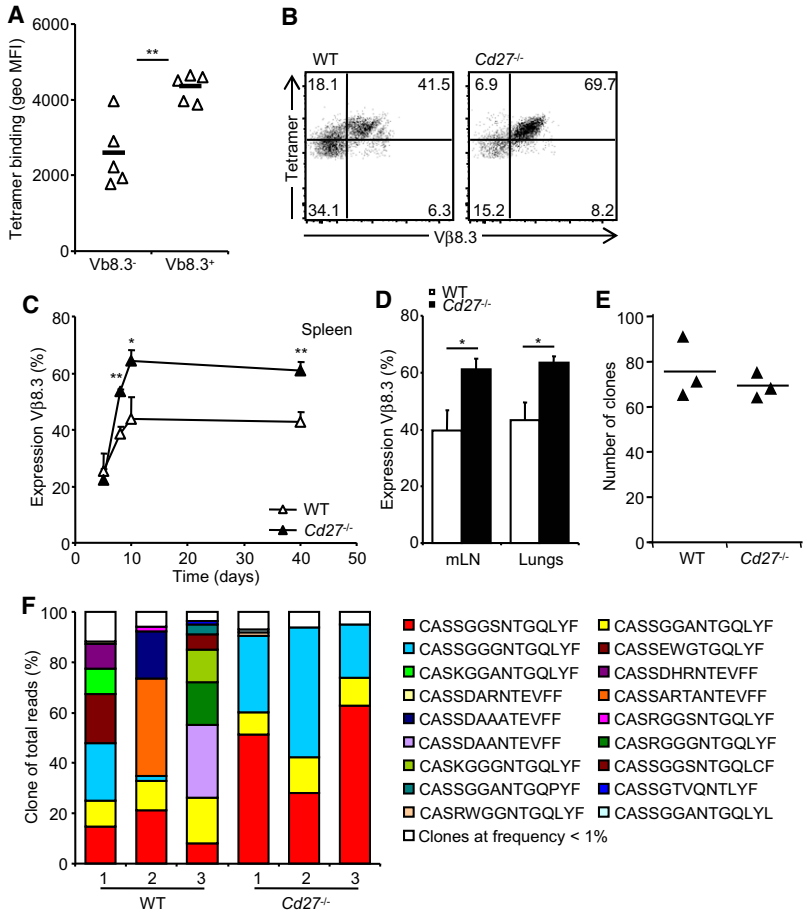

Figure 6. CD27 Favors Subdominant Clones within the Virus-Specific CD8+ T Cell Pool

WT and *Cd27*$^{-/-}$ mice were infected with A/PR8/34.

(A) The amount of tetramer binding was determined in Vβ8.3^{-} and Vβ8.3^{+} influenza-specific CD8^{+} T cells of WT spleen at day 10 after infection.

(B) Representative dot plots display tetramer and Vβ8.3 expression of influenza-specific CD8^{+} T cells in spleen of WT and *Cd27*$^{-/-}$ mice. Insets represent percentage of cells within quadrant.

(C) The usage of Vβ8.3 was followed over time in the influenza-specific CD8^{+} T cell population of WT and *Cd27*$^{-/-}$ spleen.

(D) The usage of Vβ8.3 was determined in mLN and lungs of WT and *Cd27*$^{-/-}$ mice at day 10 after infection.

(E and F) Influenza-specific CD8^{+} T cells were isolated 28 days after infection and analyzed with deep sequencing for TCR repertoire within the Vβ8.3 segment.

(E) The total number of different clones within this CD8^{+} T cell population was determined for WT and *Cd27*$^{-/-}$ mice.

(F) The relative frequency of influenza-specific CD8^{+} T cell clones with a frequency of higher than 1% of the total pool was analyzed within individual WT and *Cd27*$^{-/-}$ mice. Error bars denote standard error of the mean (SEM). See also Figure S6 and Table S1.

encounters with slightly modified pathogens can be anticipated as a likely event in the case of influenza due to its high mutation rate and seasonal variability.

DISCUSSION

We have addressed the role of costimulation through CD27 in polyclonal CD8^{+} T cell responses, in which competition between low- and high-affinity clones forms an essential aspect that is not taken into account by analyzing monoclonal TCR transgenic T cell populations. We show that CD27-derived signals play an essential role in the maintenance of low-affinity CD8^{+} T cells at the expense of high-affinity CD8^{+} T cells upon primary infection. This resulted in the generation of a clonally diverse CD8^{+} T cell memory pool of overall low-affinity and enabled strong secondary CD8^{+} T cell responses upon subsequent encounter with a distinct influenza virus.

In our hands CD27 was not essential for the development of effector CD8^{+} T cell responses after influenza infection, which apparently contradicts previous reports that describe that CD27 regulates the size of the influenza-specific CD8^{+} T cell response (Hendriks et al., 2000; Peperzak et al., 2010). In these studies, the NT/60/68 strain that may have different characteristics from the influenza strains HKx31, HK2/68, and A/PR8/34 that we employed was used. Moreover, we used influenza strains that were grown on mammalian cell lines and that have higher virulence than viruses grown on chicken eggs. These variations may translate into differences in antigenic load, which may critically affect costimulation (Acuto and Michel, 2003; Kündig et al., 1996). Indeed, costimulation through CD27 was particularly beneficial upon stimulation of CD8^{+} T cells under conditions of low antigenic strength, but detrimental under conditions of high antigenic strength. Previously, it has been described that the costimulatory effect of CD27 is mediated at least in part by the prosurvival molecule Bcl-Xl and independently by the induction of IL-2 (Peperzak et al., 2010; van Oosterwijk et al., 2007). These pathways may account for the beneficial effects of CD27-driven costimulation that we observe under low antigenic triggering. CD27-induced apoptosis specifically occurs under high antigenic triggering and probably involves the Fas and FasL system (Arens et al., 2005). The opposite effects of CD27-driven costimulation under high and low antigenic triggering are consistent with the idea that CD27 directs immune responses toward an optimum (Nolte et al., 2009).

Endogenous CD8^{+} T cell responses are suppressed by injection of TCR transgenic T cells of high-antigen affinity, suggesting that CD8^{+} T cells compete for antigen, thereby resulting in the preferential outgrowth of high-affinity clones (Butz and Bevan, 1998; Smith et al., 2000). This is beneficial in primary infection because it favors the outgrowth of an effector CD8^{+} T cell population of high-affinity clones that is superiorly equipped to combat infection. Competition does not result in complete exclusion of low-affinity clones, given that these can participate at low numbers in T cell responses (Malherbe et al., 2004; Zehn et al., 2009). We have shown here that CD27-driven costimulation played a key role in the maintenance of particularly low-affinity CD8^{+} T cells during in vivo responses. This was

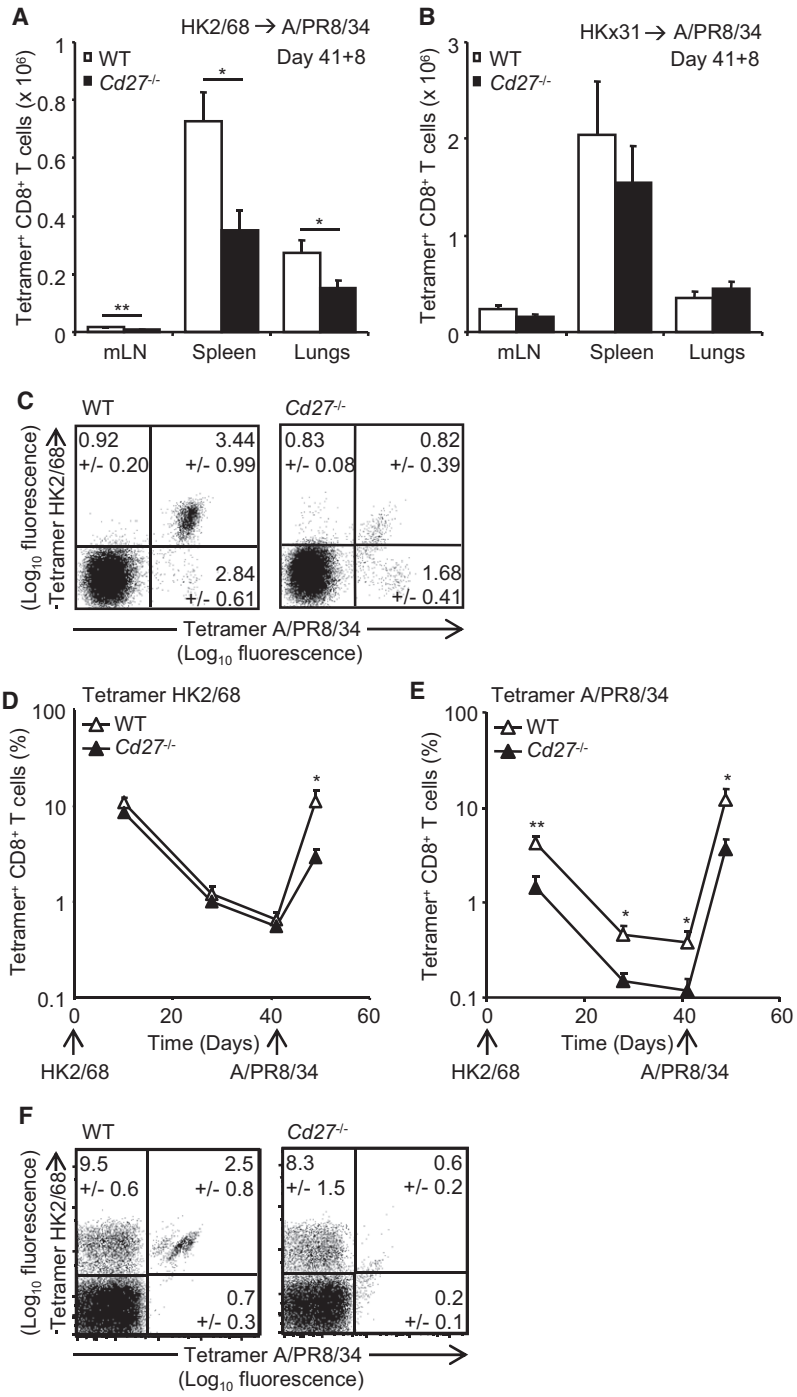

Figure 7. CD8+ T Cell Responses upon Rechallenge with Heterologous but Not Homologous Virus Require CD27

(A) WT and *Cd27*$^{-/-}$ mice were sequentially infected with the heterologous viruses HK2/68 and 41 days later A/PR8/34. The absolute numbers of influenza-specific CD8+ T cells were determined in mLN, spleen and lungs of WT and *Cd27*$^{-/-}$ mice 8 days after re-challenge using A/PR8/34 specific tetramers.

(B) WT and *Cd27*$^{-/-}$ mice were infected with HKx31 and after 41 days the mice were rechallenged with the homologous virus A/PR8/34. The influenza-specific CD8+ T cell population was quantified in the mLN, the spleen, and lungs of WT and *Cd27*$^{-/-}$ mice 8 days after rechallenge with A/PR8/34 specific tetramers.

(C) Mice were infected as described under (A). Representative dotplots are shown of CD8+ T cells of WT (left) and *Cd27*$^{-/-}$ spleen (right) displaying costaining for A/PR8/34 and HK2/68 specific tetramers. Insets represent the mean ± SEM of the percentages of cells within the respective quadrants. The percentage of cells in upper right quadrant is significantly different between WT and *Cd27*$^{-/-}$ mice ($p < 0.05$).

(D and E) The frequency of CD8+ T cells recognizing HK2/68 specific tetramers (D) and those cross-reactive with A/PR8/34 specific tetramers (E) was followed in time upon HK2/68 infection (at day 0) and A/PR8/34 reinfection (at day 41) in the blood of WT and *Cd27*$^{-/-}$ mice. Arrowheads indicate time of influenza infection.

(F) Mice were infected with HK2/68 and analyzed 10 days later. Representative dot plots are shown of CD8+ T cells of WT (left) and *Cd27*$^{-/-}$ blood (right) displaying costaining for tetramers specific for HK2/68 and A/PR8/34. Insets represent the mean ± SEM of the percentages of cells within the respective quadrants. The percentage of cells in upper-right quadrant is significantly different between WT and *Cd27*$^{-/-}$ mice ($p < 0.05$). Error bars denote standard error of the mean (SEM). See also Figure S7.

supported by in vitro findings showing that the beneficial effects of CD27-driven costimulation increased when the avidity of the TCR-antigen interaction decreased. Our mixed BM-chimeric mice revealed that CD27 on CD8+ T cells rather than on CD4+ T cells or any other cell type was essential for inducing autocrine IL-2 production and for mediating survival of low-affinity clones. IL-2 signaling promotes effector differentiation in CD8+ T cells that sustain expression of CD25 (Kalia et al., 2010; Pipkin et al., 2010). High expression of CD25 provides a competitive advantage for effector CD8+ T cell clones specifically upon stimulation with high-affinity antigen (Wensveen et al., 2010; Zehn et al., 2009). In contrast, by providing IL-2, CD27 may reduce antigen requirements to allow expansion and differentiation of low-affinity CD8+ T cell clones. This idea is consistent with the finding that CD27-driven costimulation specifically enhanced differentiation of low-affinity CD8+ T cells into EM precursors and terminal effectors.

CD27 uses signaling components that overlap with those of related members of the TNFR superfamily such as HVEM, 4-1BB, CD30, and OX40, indicating that IL-2 may also be induced after ligation of these receptors (Croft, 2009; Nolte et al., 2009). Furthermore, induction of IL-2 production is a central feature of CD28 costimulation (Acuto and Michel, 2003), making a role for this costimulatory pathway in the affinity regulation of CD8+ T cells similar to CD27 conceivable. Indeed, costimulation through CD28 lowers the threshold of activation and enables individual CD8+ T cells to respond to lower amounts of antigen and or to low-avidity antigens (Viola and Lanzavecchia, 1996).

CD27-dependent maintenance of low-affinity CD8+ T cells correlated with CD27-dependent preservation of a more diverse memory pool at the level of Vβ usage and at the clonal level within the dominant Vβ population. This infers that CD27-driven costimulation is vital for the maintenance of multiple subdominant CD8+ T cell clones that are of lower affinity than the dominant clone. In the absence of CD27, competition is likely stronger, which may account for the outgrowth of only a limited set of dominant clones of high affinity. CD27 did not increase antigen affinity or usage of the dominant Vβ within CM-type MPECs. Interestingly, CM-type MPECs display a higher degree of clonal diversity than EM-type MPECs or SLECs (Kedzierska et al., 2006). These differences in CD8+ T cell repertoire persist into the memory phase, given that CM CD8+ T cells are more clonally diverse than EM CD8+ T cells (Kedzierska et al., 2006). Such low-affinity CM-type MPECs probably require antigen-independent survival signals to face competition with high-affinity clones. CD27 did not provide survival signals for CM-type MPECs, but may promote the outgrowth and differentiation of CM-type MPECs to enhance clonal diversity in the EM-type MPEC and SLEC compartment and ultimately in the EM compartment.

A clonally diverse memory pool is likely to contain cross-reactive CD8+ T cell clones that are of potential use upon reinfection with heterologous viruses. Indeed, CD27 enhanced the degree of cross-reactivity in influenza-specific CD8+ T cells upon primary infection, which resulted in a better response upon secondary encounter with a heterologous virus. Our data suggested that cross-reactivity within the CD8+ T cell pool resided in one or a few of the subdominant clones. As the generation of cross-reactive clones upon influenza infection is a stochastic process, CD27-driven costimulation would increase the likelihood for the outgrowth of such a clone by allowing the coexistence of more subdominant memory CD8+ T cell clones. Thus, an important reason for the maintenance of clonal diversity by CD27 may be to ensure the presence of cross-reactive clones within the memory CD8+ T cell compartment. By demonstrating that maintenance of low-affinity CD8+ T cells is an active process that requires CD27-dependent costimulation, we argue that memory may in fact be a strategy to cost-effectively invest in CD8+ T cell clones that have higher potential than the naive compartment against viral variants.

The resolution of viral infection correlates with broad CD8+ T cell responses, whereas viral persistence corresponds with narrow CD8+ T cell responses (Posnett et al., 2005). Therefore, strategies that aim to improve clonal diversity of CD8+ T cell responses may form a promising approach in vaccine development (Posnett et al., 2005). Our findings demonstrate that costimulation through CD27 may prove a tool in vaccine design to widen the effector CD8+ T cell repertoire and enable multipronged CD8+ T cell-mediated protection against infection or tumors.

EXPERIMENTAL PROCEDURES

Mice

C57Bl/6/J WT, Ly5.1, OTI Tg (from Jackson Laboratory), *Cd27*$^{-/-}$ (Hendriks et al., 2000) *Cd27*$^{-/-}$ × OTI Tg and *Cd27*$^{-/-}$ × CD70 Tg mice (Arens et al., 2001) were maintained at SPF conditions at the animal department of the AMC (Amsterdam, Netherlands). Mice were used at 8–12 weeks of age and within individual experiments mice were matched for age and gender. We generated mixed BM chimeras containing WT and *Cd27*$^{-/-}$ BM in a 1:1 ratio by lethally irradiating (2 × 5 Gy) WT BM recipients and reconstituting them by intravenous injection of 2 × 10^7 donor BM cells. Cells of host and WT and *Cd27*$^{-/-}$ donor origin were identified with the congenic Ly5.1/2 markers. Mixed BM chimeras were used 12 weeks after engraftment. All animal experiments were performed according institutional and national guidelines.

Antibodies

The following monoclonal antibodies from eBioscience or BD were used: anti-CD3 (145-2C11), anti-CD4 (RM4-5), anti-CD8 (53-6.7), anti-CD25 (PC61.5), anti-CD43 (1B11), anti-CD44 (IM7), anti-Ly5.1 (A20), anti-Ly5.2 (104), anti-CD62L (MEL-14), anti-CD70 (FR70), anti-CD80 (16-10A1), anti-CD86 (GL1), anti-CD127 (A7R34), anti-MHC class I (28-14-8), anti-Vβ8.3 (CT 8C1), anti-Vβ11 (RR3-15), anti-IFN-γ (XMG1.2), and anti-IL-2 (JES6-5H4).

Influenza Infection

Mice were intranasally infected either with 10× $TCID_{50}$ of the H1N1 influenza A virus A/PR8/34 or 100× $TCID_{50}$ of the H3N2 virus HK2/68. We obtained stocks and viral titers by infecting MDCK or LLC-MK2 cells as described (Bodewes et al., 2009; van der Sluijs et al., 2004). For homologous secondary CD8+ T cell responses, mice were sequentially infected with 100× $TCID_{50}$ of the H3N2 virus HKx31 and 100x $TCID_{50}$ of A/PR8/34. For heterologous secondary CD8+ T cell responses, mice were sequentially infected with 100× $TCID_{50}$ of HK2/68 and 100× $TCID_{50}$ of A/PR8/34. The use of viruses that contain distinct external epitopes, such as HK2/68 and HKx31 versus A/PR8/34, in sequential infection of the mice prevents rapid clearance of the secondary virus by neutralizing antibodies. At the indicated days after infection, mice were sacrificed and organs were harvested.

Flow Cytometry

Single-cell suspensions were obtained from spleen, mLNs, and lungs by grinding tissue over nylon filters (BD Biosciences). Erythrocytes were removed with erylysis buffer (155 mM NH_4Cl, 10 mM $KHCO_3$, and 1 mM EDTA) and cell counts were determined by an automated cell counter (CasyCounter, Innovatis). Cells were stained with fluorochrome-conjugated primary antibodies in the presence of anti-CD16/CD32 block (2.4G2) for 30 min at 4°C in PBS containing 0.5% BSA. Influenza-specific CD8+ T cells were enumerated with anti-CD8 antibodies and PE- or APC-conjugated tetramers of H-$2D^b$ containing the influenza-derived peptide $NP_{366-374}$ ASNENMETM for the influenza strains A/PR8/34 and HKx31 or ASNENMDAM for the influenza strain HK2/68. Expression was measured with Calibur or Canto flow cytometers (BD Biosciences).

Intracellular Cytokine Staining

Splenocytes were restimulated with the influenza-specific peptide ASNENMETM for 4 hr in the presence of 10 μg/ml brefeldin A (Sigma) for prevention of cytokine release. Then, splenocytes were stained with antibodies against CD4 and CD8, fixed and permeabilized using Cytofix/Cytoperm (BD Biosciences) and labeled with IFN-γ and IL-2 specific antibodies.

Analysis of T Cell Repertoire

Total RNA was extracted from tetramer sorted CD8+ T cells using Trizol (Invitrogen) isolation. cDNA was generated with SuperscriptII-RT and hexamer primers (Invitrogen). TCRs of the tetramer-specific cells were amplified with a primer specific for the Vβ8.3 gene segment (5′-TGCTGGCAACCTTCGAA TAGGA-3′) and a primer specific for the constant segment (5′-AAGGAG ACCTTGGGTGGAGT-3′). Amplification products were purified with AMPure SPRI beads (Agencourt Bioscience). The CDR3 of the β-chain was used as a unique tag for clonal expansions (Klarenbeek et al., 2010). Sequencing was performed in accordance with the manufacturer's protocol for amplicon sequencing on the FLX platform (Roche Diagnostics).

In Vitro T Cell Stimulation

OTI cells were isolated from spleen with anti-CD8 coated microbeads (Miltenyi Biotec) and labeled with CFSE (Molecular Probes). Splenocytes of *Cd27*$^{-/-}$ mice (referred to as control APCs) or *Cd27*$^{-/-}$ × CD70 Tg mice (referred to as CD70 Tg APCs) were used as APCs after irradiation (30 Gray) and labeling with DDAO (Molecular Probes). OTI cells were stimulated in 96-well

round-bottom plates (Corning) with the indicated concentrations of peptide and in the presence of APCs in a 1:1 ratio. After 3 days, proliferation of $DDAO^{-}$ $CD8^{+}$ T cells was measured with CFSE dilution and cell death by staining for propidium iodide (Molecular Probes).

Statistical Analysis

Figures represent means and error bars denote standard error of the mean (SEM). Student's t test was used for analyzing for statistical significance. $p < 0.05$ was considered statistically significant; $^{*}p < 0.05$ and $^{**}p < 0.005$. Experimental groups consisted of three to nine mice and all experiments have been performed twice unless indicated otherwise.

SUPPLEMENTAL INFORMATION

Supplemental Information includes seven figures and one table and can be found with this article online at doi:10.1016/j.immuni.2011.04.020.

ACKNOWLEDGMENTS

We thank A. de Bruin for technical assistance, B. Hooibrink for cell sorting, G. van Schijndel for tetramer production, B. van Schaik and A. van Kampen for statistical analysis, and the staff of the animal facility of the AMC for excellent animal care. We thank L. Boon, R. Bodewes, and G. Rimmelzwaan for kindly providing reagents. Finally, we thank J. Borst, N. de Vries, E. van Leeuwen, and M. Wolkers for critical reading of the manuscript and helpful discussion. This study was supported by an LSBR grant (NAMK), a VIDI Grant (MAN), and a VICI Grant (RAWvL) from The Netherlands Organization of Scientific Research.

Received: October 26, 2010
Revised: February 21, 2011
Accepted: April 20, 2011
Published online: July 14, 2011

REFERENCES

Acuto, O., and Michel, F. (2003). CD28-mediated co-stimulation: A quantitative support for TCR signalling. Nat. Rev. Immunol. *3*, 939–951.

Arens, R., Tesselaar, K., Baars, P.A., van Schijndel, G.M., Hendriks, J., Pals, S.T., Krimpenfort, P., Borst, J., van Oers, M.H., and van Lier, R.A. (2001). Constitutive CD27/CD70 interaction induces expansion of effector-type T cells and results in IFNgamma-mediated B cell depletion. Immunity *15*, 801–812.

Arens, R., Baars, P.A., Jak, M., Tesselaar, K., van der Valk, M., van Oers, M.H., and van Lier, R.A. (2005). Cutting edge: CD95 maintains effector T cell homeostasis in chronic immune activation. J. Immunol. *174*, 5915–5920.

Badovinac, V.P., Messingham, K.A., Jabbari, A., Haring, J.S., and Harty, J.T. (2005). Accelerated $CD8^{+}$ T-cell memory and prime-boost response after dendritic-cell vaccination. Nat. Med. *11*, 748–756.

Belz, G.T., Bedoui, S., Kupresanin, F., Carbone, F.R., and Heath, W.R. (2007). Minimal activation of memory $CD8^{+}$ T cell by tissue-derived dendritic cells favors the stimulation of naive $CD8^{+}$ T cells. Nat. Immunol. *8*, 1060–1066.

Bodewes, R., Kreijtz, J.H., Baas, C., Geelhoed-Mieras, M.M., de Mutsert, G., van Amerongen, G., van den Brand, J.M., Fouchier, R.A., Osterhaus, A.D., and Rimmelzwaan, G.F. (2009). Vaccination against human influenza A/H3N2 virus prevents the induction of heterosubtypic immunity against lethal infection with avian influenza A/H5N1 virus. PLoS ONE *4*, e5538.

Brehm, M.A., Pinto, A.K., Daniels, K.A., Schneck, J.P., Welsh, R.M., and Selin, L.K. (2002). T cell immunodominance and maintenance of memory regulated by unexpectedly cross-reactive pathogens. Nat. Immunol. *3*, 627–634.

Butz, E.A., and Bevan, M.J. (1998). Massive expansion of antigen-specific $CD8^{+}$ T cells during an acute virus infection. Immunity *8*, 167–175.

Carr, J.M., Carrasco, M.J., Thaventhiran, J.E., Bambrough, P.J., Kraman, M., Edwards, A.D., Al-Shamkhani, A., and Fearon, D.T. (2006). CD27 mediates interleukin-2-independent clonal expansion of the $CD8^{+}$ T cell without effector differentiation. Proc. Natl. Acad. Sci. USA *103*, 19454–19459.

Chang, J.T., Palanivel, V.R., Kinjyo, I., Schambach, F., Intlekofer, A.M., Banerjee, A., Longworth, S.A., Vinup, K.E., Mrass, P., Oliaro, J., et al. (2007). Asymmetric T lymphocyte division in the initiation of adaptive immune responses. Science *315*, 1687–1691.

Cornberg, M., Chen, A.T., Wilkinson, L.A., Brehm, M.A., Kim, S.K., Calcagno, C., Ghersi, D., Puzone, R., Celada, F., Welsh, R.M., and Selin, L.K. (2006). Narrowed TCR repertoire and viral escape as a consequence of heterologous immunity. J. Clin. Invest. *116*, 1443–1456.

Croft, M. (2009). The role of TNF superfamily members in T-cell function and diseases. Nat. Rev. Immunol. *9*, 271–285.

Gerlach, C., van Heijst, J.W., Swart, E., Sie, D., Armstrong, N., Kerkhoven, R.M., Zehn, D., Bevan, M.J., Schepers, K., and Schumacher, T.N. (2010). One naive T cell, multiple fates in $CD8^{+}$ T cell differentiation. J. Exp. Med. *207*, 1235–1246.

Haanen, J.B., Wolkers, M.C., Kruisbeek, A.M., and Schumacher, T.N. (1999). Selective expansion of cross-reactive $CD8(^{+})$ memory T cells by viral variants. J. Exp. Med. *190*, 1319–1328.

Harty, J.T., and Badovinac, V.P. (2008). Shaping and reshaping $CD8^{+}$ T-cell memory. Nat. Rev. Immunol. *8*, 107–119.

Hendriks, J., Gravestein, L.A., Tesselaar, K., van Lier, R.A., Schumacher, T.N., and Borst, J. (2000). CD27 is required for generation and long-term maintenance of T cell immunity. Nat. Immunol. *1*, 433–440.

Huster, K.M., Busch, V., Schiemann, M., Linkemann, K., Kerksiek, K.M., Wagner, H., and Busch, D.H. (2004). Selective expression of IL-7 receptor on memory T cells identifies early CD40L-dependent generation of distinct $CD8^{+}$ memory T cell subsets. Proc. Natl. Acad. Sci. USA *101*, 5610–5615.

Kaech, S.M., Tan, J.T., Wherry, E.J., Konieczny, B.T., Surh, C.D., and Ahmed, R. (2003). Selective expression of the interleukin 7 receptor identifies effector CD8 T cells that give rise to long-lived memory cells. Nat. Immunol. *4*, 1191–1198.

Kalia, V., Sarkar, S., Subramaniam, S., Haining, W.N., Smith, K.A., and Ahmed, R. (2010). Prolonged interleukin-2Ralpha expression on virus-specific CD8+ T cells favors terminal-effector differentiation in vivo. Immunity *32*, 91–103.

Kedzierska, K., Turner, S.J., and Doherty, P.C. (2004). Conserved T cell receptor usage in primary and recall responses to an immunodominant influenza virus nucleoprotein epitope. Proc. Natl. Acad. Sci. USA *101*, 4942–4947.

Kedzierska, K., Venturi, V., Field, K., Davenport, M.P., Turner, S.J., and Doherty, P.C. (2006). Early establishment of diverse T cell receptor profiles for influenza-specific $CD8(^{+})CD62L(^{hi})$ memory T cells. Proc. Natl. Acad. Sci. USA *103*, 9184–9189.

Kedzierska, K., Stambas, J., Jenkins, M.R., Keating, R., Turner, S.J., and Doherty, P.C. (2007). Location rather than CD62L phenotype is critical in the early establishment of influenza-specific $CD8^{+}$ T cell memory. Proc. Natl. Acad. Sci. USA *104*, 9782–9787.

Kedzierska, K., Thomas, P.G., Venturi, V., Davenport, M.P., Doherty, P.C., Turner, S.J., and La Gruta, N.L. (2008). Terminal deoxynucleotidyltransferase is required for the establishment of private virus-specific $CD8^{+}$ TCR repertoires and facilitates optimal CTL responses. J. Immunol. *181*, 2556–2562.

Klarenbeek, P.L., Tak, P.P., van Schaik, B.D., Zwinderman, A.H., Jakobs, M.E., Zhang, Z., van Kampen, A.H., van Lier, R.A., Baas, F., and de Vries, N. (2010). Human T-cell memory consists mainly of unexpanded clones. Immunol. Lett. *133*, 42–48.

Kündig, T.M., Shahinian, A., Kawai, K., Mittrücker, H.W., Sebzda, E., Bachmann, M.F., Mak, T.W., and Ohashi, P.S. (1996). Duration of TCR stimulation determines costimulatory requirement of T cells. Immunity *5*, 41–52.

Lenschow, D.J., Walunas, T.L., and Bluestone, J.A. (1996). CD28/B7 system of T cell costimulation. Annu. Rev. Immunol. *14*, 233–258.

Malherbe, L., Hausl, C., Teyton, L., and McHeyzer-Williams, M.G. (2004). Clonal selection of helper T cells is determined by an affinity threshold with no further skewing of TCR binding properties. Immunity *21*, 669–679.

Nolte, M.A., van Olffen, R.W., van Gisbergen, K.P., and van Lier, R.A. (2009). Timing and tuning of CD27-CD70 interactions: The impact of signal strength in setting the balance between adaptive responses and immunopathology. Immunol. Rev. *229*, 216–231.

Peperzak, V., Xiao, Y., Veraar, E.A., and Borst, J. (2010). CD27 sustains survival of CTLs in virus-infected nonlymphoid tissue in mice by inducing autocrine IL-2 production. J. Clin. Invest. *120*, 168–178.

Pipkin, M.E., Sacks, J.A., Cruz-Guilloty, F., Lichtenheld, M.G., Bevan, M.J., and Rao, A. (2010). Interleukin-2 and inflammation induce distinct transcriptional programs that promote the differentiation of effector cytolytic T cells. Immunity *32*, 79–90.

Posnett, D.N., Engelhorn, M.E., and Houghton, A.N. (2005). Antiviral T cell responses: Phalanx or multipronged attack? J. Exp. Med. *201*, 1881–1884.

Prlic, M., Williams, M.A., and Bevan, M.J. (2007). Requirements for CD8 T-cell priming, memory generation and maintenance. Curr. Opin. Immunol. *19*, 315–319.

Smith, A.L., Wikstrom, M.E., and Fazekas de St Groth, B. (2000). Visualizing T cell competition for peptide/MHC complexes: A specific mechanism to minimize the effect of precursor frequency. Immunity *13*, 783–794.

Stemberger, C., Huster, K.M., Koffler, M., Anderl, F., Schiemann, M., Wagner, H., and Busch, D.H. (2007). A single naive CD8+ T cell precursor can develop into diverse effector and memory subsets. Immunity *27*, 985–997.

van der Sluijs, K.F., van Elden, L.J., Nijhuis, M., Schuurman, R., Pater, J.M., Florquin, S., Goldman, M., Jansen, H.M., Lutter, R., and van der Poll, T. (2004). IL-10 is an important mediator of the enhanced susceptibility to pneumococcal pneumonia after influenza infection. J. Immunol. *172*, 7603–7609.

van Oosterwijk, M.F., Juwana, H., Arens, R., Tesselaar, K., van Oers, M.H., Eldering, E., and van Lier, R.A. (2007). CD27-CD70 interactions sensitise naive CD4+ T cells for IL-12-induced Th1 cell development. Int. Immunol. *19*, 713–718.

Viola, A., and Lanzavecchia, A. (1996). T cell activation determined by T cell receptor number and tunable thresholds. Science *273*, 104–106.

Wensveen, F.M., van Gisbergen, K.P., Derks, I.A., Gerlach, C., Schumacher, T.N., van Lier, R.A., and Eldering, E. (2010). Apoptosis threshold set by Noxa and Mcl-1 after T cell activation regulates competitive selection of high-affinity clones. Immunity *32*, 754–765.

Xiao, Y., Peperzak, V., Keller, A.M., and Borst, J. (2008). CD27 instructs CD4+ T cells to provide help for the memory CD8+ T cell response after protein immunization. J. Immunol. *181*, 1071–1082.

Zehn, D., Lee, S.Y., and Bevan, M.J. (2009). Complete but curtailed T-cell response to very low-affinity antigen. Nature *458*, 211–214.